Available online at www.sciencedirect.com
ScienceDirect
Dyes and Pigments 76 (2008) 422–428
DYES and PIGMENTS
www.elsevier.com/locate/dyepig

Crystal morphology and their lattice contraction control for the topochemical reaction of bis(phenylethenyl)-dicyanopyrazines

Jae Hong Kim [a,*], Young Chul Choi [a], Bong Shik Kim [a], Dong Hoon Choi [b], Sung Hoon Kim [c]

[a] School of Chemical Engineering and Technology, Yeungnam University, 214-1, Dae-dong, Gyeongsan, Gyeongbuk 712-749, South Korea
[b] Department of Chemistry, Korea University, Seoul 136-701, South Korea
[c] Department of Textile System Engineering, Kyungpook National University, Daegu 702-701, South Korea

Received 1 April 2006; received in revised form 25 May 2006; accepted 12 September 2006
Available online 28 November 2006

Abstract

Topochemical photoreaction of bis(phenylethenyl)-dicyanopyrazines (**1**) was conducted in solution, in the vapor deposited thin film, and in the single crystals. Compound **1** showed the crystal morphology to give the yellow and orange colored crystals. The difference in crystal structures of yellow and orange crystals was confirmed with X-ray crystal analysis which revealed that the orange one was contracted in the crystallographic *c*-axis by 0.11 Å than that of the yellow one at the same temperature. The physical property and photoreactivity of two crystals were explained with the topochemical control and lattice contraction.

Keywords: Topochemical photoreaction; Crystal morphology; Lattice contraction; Intermolecular interaction

1. Introduction

Solid-state chemistry of organic materials is of current interest with respect to their functionalities for electronics and photonics due to the molecular stacking in aggregates [1,2]. Many functionalities of organic materials are induced from π-electron oriented intermolecular interactions which can control such diverse phenomena as the intercalation of drugs into DNA, the packing of aromatic molecules in crystals, the complexation in host–guest systems and porphyrin aggregation, supramolecular chemistry [3–7]. Dye molecules have a large π-conjugated planar structure and are thus promising candidates for organic functional materials. We have reported that the self-assembling characteristics of some naphthoquinone dyes which revealed strong three-dimensional molecular stacking in the solid state and gave large 3rd order nonlinear optical susceptibility. Intermolecular π–π interactions due to strong molecular stacking are very significant to induce special functionalities in the solid state such as reactivity, conductivity, and photoconductivity [8–12].

On the other hand, solid-state chemical reactions, despite the great potential advantages of enhanced stereo- and regioselectivity [13], environmental-friendly solvent-free conditions [14], and high crystallinity of the products [15–17], still remain rather limited in practical applications. In the solid-state photoreaction, so-called topochemical control is generally known in which the crystal structures and the distance between the reactive centers determine the reactivity and stereochemical structure of products because limited motions of molecules in the crystal state were proposed in comparison with those in solution [18–21]. Recent studies on the photodimerization of olefinic crystals have revealed that the reactivity of crystals was related with the free space around the reaction site in the crystal lattice. The terms, ‘‘space cavity’’ and ‘‘steric compression control’’ were suggested to explain the solid-state photochemical reactions [22–24]. A number of lattice-energy

* Corresponding author.
E-mail address: jaehkim@ynu.ac.kr (J.H. Kim).

0143-7208/$ - see front matter © 2006 Elsevier Ltd. All rights reserved.
doi:10.1016/j.dyepig.2006.09.009

calculations [25] and the kinetic study [16,26] were carried out to understand reactivities of olefinic crystalline compounds and the results were in good agreement with experimental observations.

In the previous paper, we have reported that the topochemical solid-state photodimerization of (phenylethenyl)-dicyanopyrazines were strongly affected by the differences in their crystal structures [27]. Photoreactivity in the solid state was controlled by topochemically allowed molecular movement in the crystal lattice which was confirmed by the X-ray crystal analysis. In this paper, we intend to clarify the specific lattice contraction with respect to intermolecular π–π interaction influencing on the photoreactivities and physical properties of 2,3-bis(phenylethenyl)-5,6-dicyanopyrazines in the solid state. We believe that this concept allows to understand many photochemical behaviors of olefinic compounds in the solid state.

2. Results

2.1. Photoreaction of bis(phenylethenyl)-dicyanopyrazines

Photoreaction of bis(phenylethenyl)-dicyanopyrazines was conducted in benzene solution, in the evaporated thin film, and in the single crystal. Benzene solution of **1a** was irradiated with 365 nm for 20 h to give the photodimer **2a** in 50% yield (Scheme 1). The resultant *anti* head-to-tail dimerized structure of **2a** was confirmed by ^{1}H NMR and mass spectra. Similar photoirradiation of **1b** in benzene solution gave a different result, yielding the mixture of **2b** and **3b** in 67% together with **4b** in 33%, with the conversion of 60%. These three products were isolated by column chromatography using ethyl acetate/*n*-hexane (v/v = 2/1) as eluent and characterized (see Section 4).

The ^{1}H NMR spectra of the cyclobutane ring protons in **2b** and **4b** are shown in Fig. 1. The different coupling patterns of the protons in the cyclobutane ring in **2b** and **4b** indicate the different stereospecific configuration of cyclobutane. The photodimer **4b** has all *trans*-coupling of protons in the cyclobutane ring and showed typical pattern in the ^{1}H NMR signal which was almost identical with photodimer having cyclobutane rings with *anti* head-to-head configuration of 1,4-dicinnamoylbenzene [28]. It means that **4b** has the layered structure having the *anti* head-to-head configuration with respect to the two cyclobutane rings. Compound **2a** (and **3b**) as well as **2b** showed AA′BB′-pattern in the NMR spectra which indicates the *anti* head-to-tail configuration in cyclobutane. Fig. 2 shows the proposed molecular pairing of **1b** in solution to give **2b** in *anti* head-to-tail form and **4b** in *anti* head-to-head form. Compounds **2b** and **3b** are geometrical isomers, which was confirmed by the coupling constants in their ^{1}H NMR spectra and reversible isomerization of **2b** and **3b** under the UV irradiation. Photoisomerization of **2b** (*trans*) to **3b** (*cis*) proceeded by irradiation with 365 nm UV light, and that of **3b** to **2b** proceeded by irradiation at 290 nm, and the isosbestic point was observed at 300 nm (Fig. 3). Consequently, the photoreaction of **1** in the solution gave three isomers having different configurations in cyclobutane and ethylene moiety.

2.2. Solid-state photoreaction of *1a* and *1b*

Compound **1a** showed the crystal morphology and gave two kinds of crystals; one is the orange colored crystal obtained from the recrystallization of **1a** from the solution of tetrahydrofuran and acetonitrile mixture (v/v = 1/1), and the other is the yellow colored crystal obtained from benzene. They showed not only different colors but also different photochemical reaction behaviors; the yellow crystal underwent polymerization in the solid state under irradiation, however, the orange one was inert photochemically. Two kinds of powdered crystals of **1a** were irradiated with 365 nm for 10 h at room temperature, separately. The yellow colored crystal of **1a** gave the insoluble photoproducts in organic solvents together with a trace amount of **2a**. However, the orange crystal did not show reaction behavior at all. Similar results were also observed in the vapor deposited thin film in which, the yellow colored film gave oligomerized products but orange colored one was quite inert (see Section 4). The vapor deposited thin film of **1a** on the quartz slide was irradiated by mercury lamp and the spectral changes in absorption and fluorescence spectra during irradiation are shown in Fig. 4. The absorbance and fluorescence intensities at around 385 nm and 520 nm, respectively, were gradually decreased with photoirradiation, indicating the cleavage of the π-conjugation of **1a** to give photoproducts.

After photobleaching of the yellow film, the product was extracted with chloroform and analyzed by gel permeation

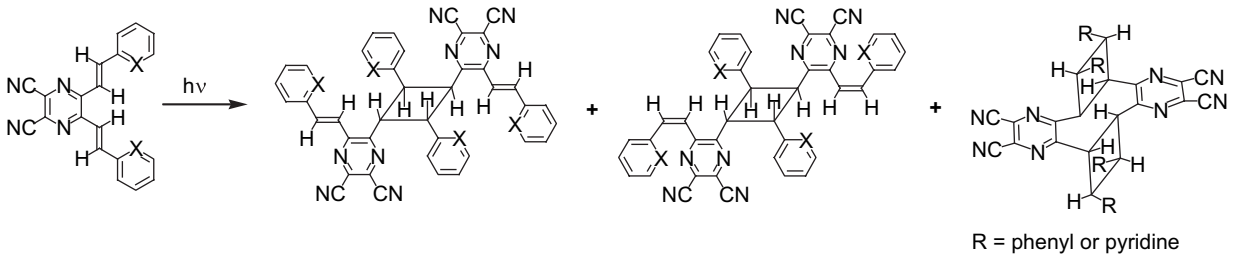

1a : X = CH
1b : X = N

2a : X = CH
2b : X = N

3a : X = CH
3b: X = N

4a : X = CH
4b : X = N

Scheme 1.

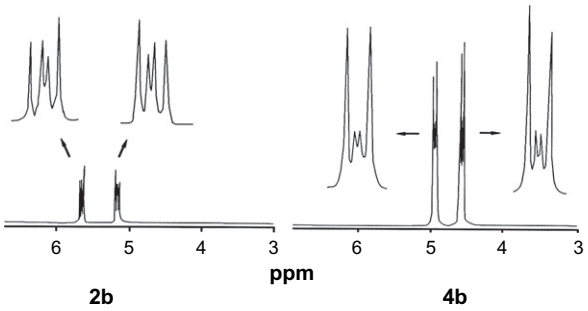

Fig. 1. The ^{1}H NMR spectra of the chemical shifts in cyclobutane of **2b** and **4b**.

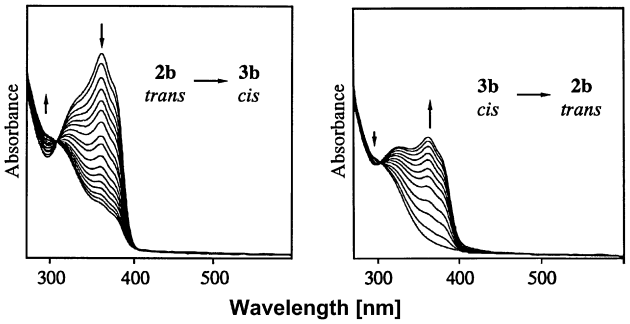

Fig. 3. The reversible photoisomerization between **2b** and **3b** in solution.

chromatography (GPC) that exhibited the clear signals at 626 and 6185 *which* correspond to the dimer and oligomer (18–19 units) of **1a**, respectively. Photoirradiation of the vapor deposited thin film of **1b** gave **2b** together with a small amount of insoluble photoproduct but did not give **3b** nor **4b**.

2.3. X-ray single crystal structure analyses

The X-ray crystal structure analyses of the two crystals (yellow and orange ones) of **1a** were carried out to confirm the differences in molecular packing structures (Table 1). The X-ray crystal analysis of yellow crystal of **1a** revealed the planar and layered molecular packing structure. The results are shown in Figs. 5 and 6.

Each molecule is oriented along the same line of direction in the plane, and the nearest next lines are oriented in the opposite direction. Alternative orientations of each line are observed in the same plane. Although the distances between the planes are calculated as 3.5 Å, the intermolecular distance of the ethylene units (reactive centers) in upper and lower molecules to give the photodimer was observed as 5.7 Å, and consequently, **2a** (*anti* head-to-tail configuration) could be obtained from the results of the lattice slipping behavior in ca. 4.5 Å in the crystal structures under photoirradiation (Fig. 6). Photo-polymerization mechanism of **1a** in the solid state was proposed as shown in Fig. 7, indicating three layered structures in the crystal lattice. If the molecule in the middle layer slipped by 4.5 Å in the plane, one of the double bonds in **1a** is overlapped in parallel with that of the molecule in the upper layer with *anti* head-to-tail configuration and simultaneously, the other double bond is overlapped with that of the lower layer in a same way for photoreaction, and consequently, photo-oligomerization and/or polymerization could proceed with the lattice slipping in the solid state.

On the other hand, the orange crystal of **1a** was photostable and its X-ray crystal analysis revealed that the orange one was contracted in the crystallographic *c*-axis by 0.11 Å in comparison with that of the yellow crystal at the same temperature (Table 1). Thus, the distance between the reactive double bonds in the orange crystal is 5.6 Å, which are closer than that in the yellow crystal. Consequently, in the orange crystal, the enhanced intermolecular interaction makes more packed dense crystal structure than yellow one, which can interrupt the molecular movement for the photoreaction.

2.4. Temperature dependence of the crystal structure of *1a*

It is known that the lattice contraction enhances the intermolecular interaction because of the lattice shrinkage [1b]. Temperature dependence of the crystal lattice changes in the two different crystals of **1a** was determined to confirm the relationship between crystal lattice contraction and photoreactivity and the results are shown in Table 1.

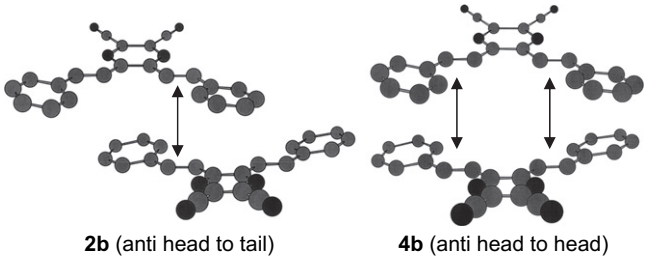

Fig. 2. Proposed molecular pairings of **1b** in solution to give **2b** and **4b**.

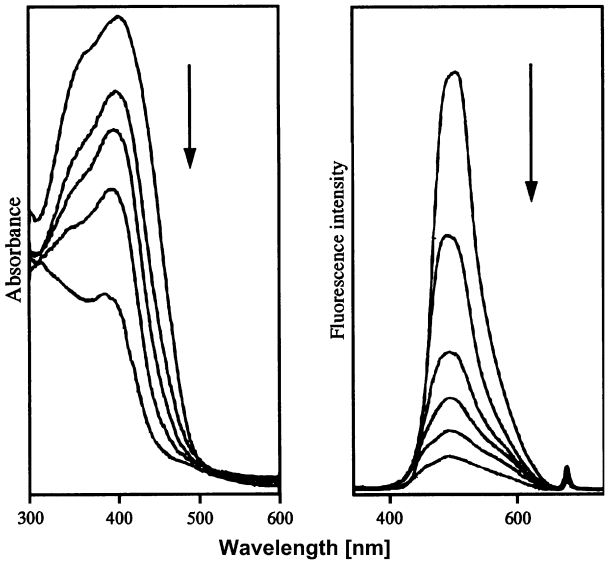

Fig. 4. Changes in the absorption (*left*) and fluorescence (*right*) spectra of **1a** on the vapor deposited thin film under irradiation (time intervals 2 min).

Table 1
Temperature dependencies in the crystal data of the yellow crystal of **1a**

Temperature (°C)	Yellow crystal		Δ[a]	Orange crystal		Δ[a]
	23[b]	−120[c]		23[b]	−120[c]	
Crystal symmetry	Monoclinic, *C*2/*c*	Monoclinic, *C*2/*c*		Monoclinic, *C*2/*c*	Monoclinic, *C*2/*c*	
Lattice parameters						
a (Å)	13.202(3)	13.275(3)	+0.073	13.192(2)	13.242(2)	+0.052
b (Å)	12.274(3)	12.256(4)	−0.018	12.263(2)	12.225(2)	−0.038
c (Å)	12.233(3)	12.006(2)	−0.227	12.126(2)	11.945(2)	−0.181
β (°)	117.38(2)	118.32(1)	+0.94	117.49(1)	118.48(1)	+0.99
D_c (g cm^{-3})	1.261	1.291	+0.030	1.276	1.307	+0.031
Z	4	4		4	4	
R	0.040	0.040		0.053	0.042	
Rw	0.036	0.060		0.074	0.066	
Goodness of fit indicator	1.87	1.30		1.80	1.47	
μ	0.609	0.79		0.78	0.78	
Double bond distance (Å)[d]	5.70	5.56	−0.14	5.60	5.54	−0.06

[a] Differences in the lattice parameters from the data at −120 °C to that at 23 °C.
[b] Measurement was conducted at 23 °C.
[c] Measurement was conducted at −120 °C.
[d] Reactive double bond separation with the *anti* head-to-tail configuration.

It is obvious that the lattice in the orange crystal was contracted by 0.11 Å along the *c*-axis only in comparison with that of the yellow one at the same temperature (23 °C), however, other parameters were not changed so much. Furthermore, the lattice parameters were changed depending on the temperature (from 23 °C to −120 °C). At the low temperature, both crystals were contracted in a similar way. However, the lattice contraction of orange crystal along the *c*-axis was smaller than that of the yellow one (see Fig. 8). It indicates that the crystal lattice of the orange one was more strongly packed along the *c*-axis, influenced by the enhanced intermolecular π−π interaction. On the contrary, the yellow crystal was packed more loosely with larger intermolecular distance (by weaker intermolecular interactions) than that in orange one. Thus, it can be contracted strongly at low temperature.

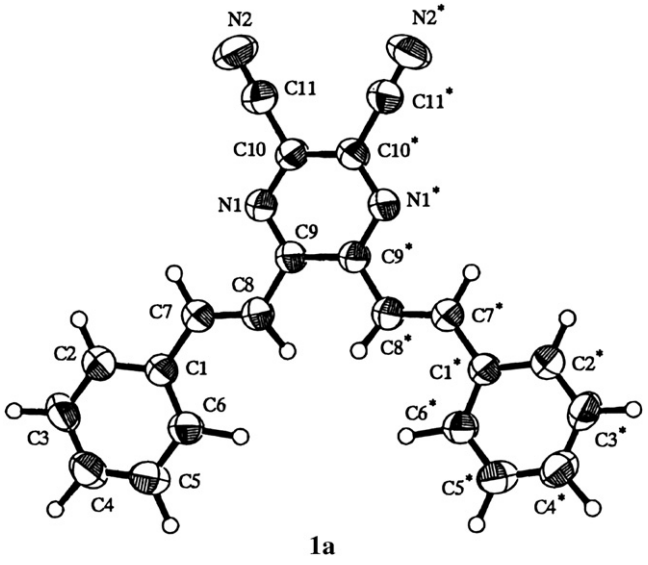

Fig. 5. The molecular structure of **1a** in the yellow crystal.

2.5. Spectral properties of yellow and orange crystals

Compound **1a** has two different crystal structures; one is orange and the other is yellow colored crystal (*vide infra*). They showed different absorption and fluorescence spectra in the solid state (yellow crystal; λ_{max}: 385 nm, F_{max}: 515 nm and

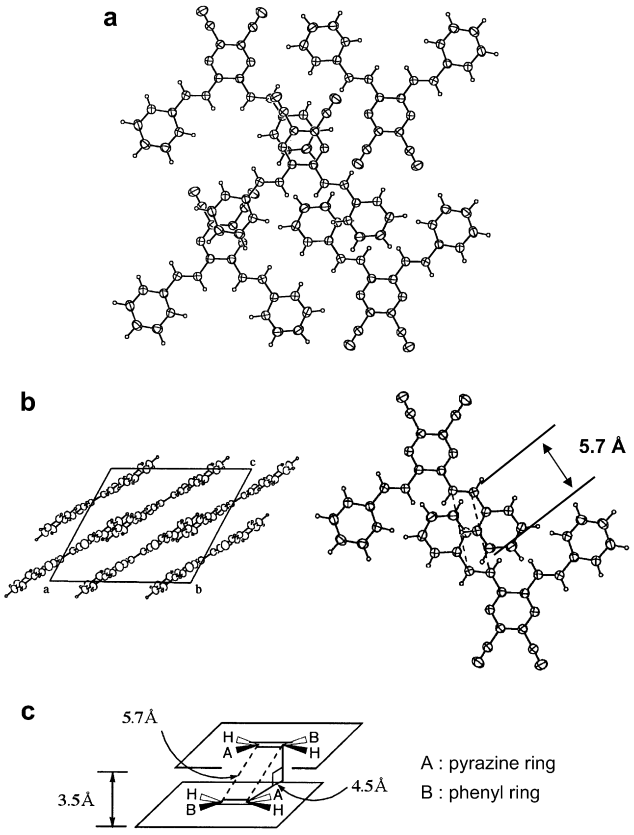

Fig. 6. The molecular packing (a and b) and the schematic representation of the photoreactive ethylene units (c) of **1a** in the yellow crystal.

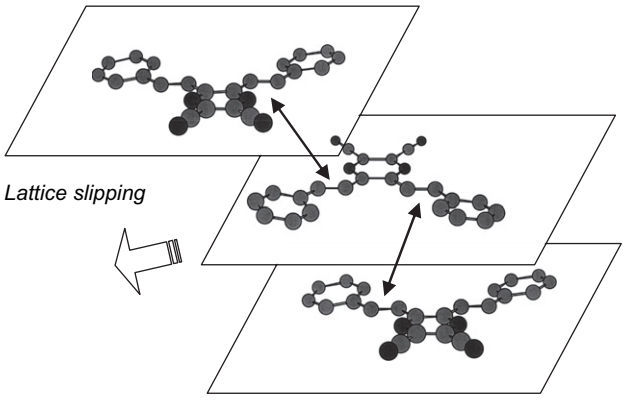

Fig. 7. Molecular stacking of **1a** in the solid state for oligomerization or polymerization under irradiation.

orange crystals; λ_{max}: 435 nm, F_{max}: 579 nm) as shown in Fig. 9. It was revealed that the orange crystal has more contracted crystal packing structure than the yellow one does by the increased intermolecular π−π interaction indicating a bathochromic shift in absorption and fluorescence spectra compared to those of the yellow one.

3. Discussion

Solid-state absorption and fluorescence spectra of organic chromophores were well correlated with their molecular stacking in aggregates or crystals [10,1b]. It has been reported that 1,4-dithioketo-3,6-diphenyl-[3,4,*c*]-pyrrole (DTPP) showed morphological transformation on exposure to certain organic solvent vapors accompanied by enhancement of photoconductivity at near infrared absorption band ($\Delta\lambda = 130$ nm). Changes in the X-ray diffraction patterns of DTPP before and after the vapor treatment indicated that small changes in the molecular stacking were occurred along with one crystallographic axis resulting in a decrease in the intermolecular

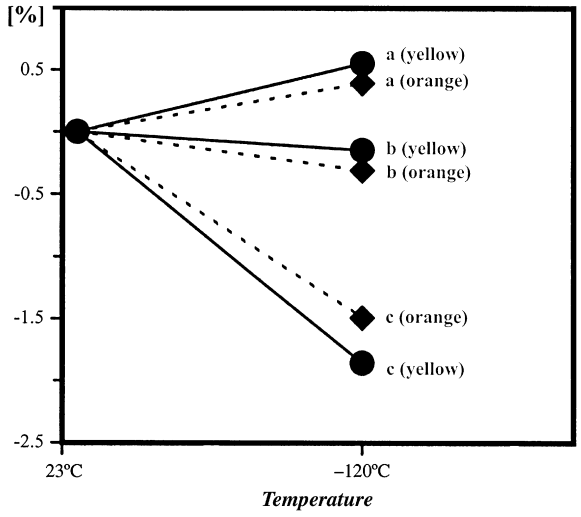

Fig. 8. Relative changes of cell parameters at the different temperatures (changes in the cell dimensions of *a*-, *b*-, and *c*-axes: a, b, and c, respectively).

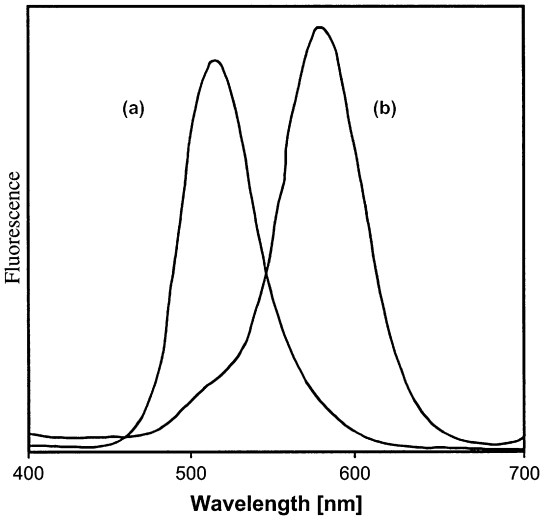

Fig. 9. Solid-state fluorescence spectra of **1a**: (a) yellow crystal; (b) orange crystal.

distances by 0.03 Å (from $2\theta = 25.20°$, $d = 3.53$ Å to 25.45°, $d = 3.50$ Å, where d denotes the intermolecular distance) [29].

In the case of **1a**, it is proposed that the orange crystals have more contracted crystal packing structure than that of the yellow one by the increased intermolecular π−π interaction which produced bathochromic shift in absorption and fluorescence spectra in comparison with those of the yellow one. The bathochromic shift of spectra was explained by the transition dipole interactions between dye molecules in aggregates [10,1b].

It is suggested that the lattice contraction to *c*-axis was strongly related with their intermolecular π−π interaction and the solid-state photoreactivities. These concepts were first stated by Schmidt and co-workers. A number of investigations in the solid-state photochemical cycloaddition of olefins have been done extensively which led to the formulation of Schmidt's criterion; the double bonds should be approximately parallel and no further than ca. 4.1 Å apart for the photodimerization to occur. They have performed pioneering works in the solid-state photodimerization of cinnamic acids [18a]. Their plenty of experimental evidence demonstrated that the intermolecular [2π + 2π] photocycloaddition proceeds inevitably as a result of favorable crystal packing arrangements; the reactive double bonds should be oriented in parallel in the distance less than 4.1 Å. However, a few exceptions have been reported, the olefinic molecules skewed at 65° in crystals were still reactive and the crystal having the reactive centers apart in 4.8 Å slipped in a lattice to give the photodimer under UV irradiation [30–32]. It is nevertheless surprising that the large molecule **1a** reacted in much longer distance of 5.7 Å in the crystals.

Furthermore, the photoreaction of yellow crystal gave oligomer and polymer as shown in Fig. 7. It means that the solid-state photocycloaddition of olefinic crystals proceeds with topochemically allowed movement of the lattice that could be considered with respect to the reaction cavity, steric compression and dynamic performances [25].

On the other hand, the orange crystal of **1a** was photostable and the X-ray crystal analysis revealed that the lattice was contracted in only crystallographic *c*-axis by 0.11 Å relative to that of yellow crystal. Thus, the distance between reactive double bonds in the orange crystal is 5.6 Å, which is closer than that in the yellow crystal.

Consequently, in the orange crystal, the enhanced intermolecular interaction makes more packed and denser crystal structure which can interrupt the molecular displacement (or lattice slipping) for the photoreaction.

4. Experimental

4.1. Materials and instruments

Compound **1** was synthesized with the known method [27] and the characterization was carried out by general procedures using the following instruments. M.p.: Yanagimoto micro melting point apparatus; uncorrected. ^{1}H NMR spectra: FT-NMR QE 300 MHz Shimadzu spectrometer; chemical shift in parts per million with reference to TMS. Mass spectra: M-80 B Hitachi mass spectrometer. UV–vis spectra: U-3410 Hitachi spectrophotometer. Gel permeation chromatography (GPC): the analyzer was composed of a Shimadzu LC-10A pump, a Shodex DEGAS KT-16 degassor, and a Sugai U-620 column oven. A combination of two polystyrene gel columns of Toso TSK gel G4000 H8 and G2500 H8 was used with chloroform as an eluent at 35 °C. The molecular weight was calibrated with respect to polystyrene standards.

4.2. Preparation of the vapor deposited thin film and single crystal

The compound was evaporated vertically from a hot plate onto the substrate (glass or quartz slide) under low pressure of about 5×10^{-6} Torr by using a vapor deposition apparatus. The distance between the sample and the substrate, and the evaporating temperature were controlled depending on the properties of the compounds. The fast evaporation of compound **1** gave a yellow colored film and slow evaporation gave an orange film, respectively. The single crystal was obtained from dilute solution by controlling the rate of evaporation of solvent. Compound **1a** gave two kinds of crystals; one is the orange colored crystal prepared from the solution in mixture of tetrahydrofuran and acetonitrile, and the other is yellow colored crystal from benzene solution. From the acetonitrile solution of **1**, the mixture of yellow and orange crystals was obtained, simultaneously.

4.3. Photoreaction in the solution

Compound **1** (1 mmol) was dissolved in benzene (20–40 ml) and the solution was irradiated with 365 nm light emitted from the high-pressure mercury lamp at room temperature for 20 h with N_2 atmosphere. The reaction mixture was evaporated to remove benzene at room temperature and each compound was separated by column chromatography using dichloromethane for **1a** and a mixture of ethyl acetate/*n*-hexane (v/v = 1/1) for **1b** as eluents, respectively.

4.4. Photoreaction in the vapor deposited thin film

The vapor deposited thin film of **1** was irradiated by 365 nm UV light for 5 h in N_2 atmosphere. The irradiated film was extracted with chloroform, and was analyzed by the gel permeation chromatography using dichloromethane as an eluent.

4.5. Photoreaction in the single crystal

Two different crystals (yellow and orange) of **1** were ground into powder and irradiated with mercury arc lamp for 10 h, separately and then, the products were suspended in chloroform and stirred overnight. The yellow crystal mainly gave insoluble photoproducts and a trace amount of **2a** in the extracted chloroform solution that was isolated by column chromatography using dichloromethane as an eluent. The orange one was inert photochemically.

4.6. Characterization of photodimer

The stereochemical assignment of **2a** was carried out from the mass spectrum, which shows *m/z* 668 (M^+) and 334 ($M^+/2$, symmetrical cleavage), while the peak corresponding to asymmetrical cleavage of cyclobutane is completely absent. The ^{1}H NMR spectrum shows two multiplets for 10 aromatic protons (centered at δ 7.69 and 7.54 ppm) and one singlet for 10H in phenyl rings tethered to the cyclobutane ring at δ 7.14. From the two doublets centered at δ 7.92 and 7.18 with $J = 15.4$ Hz for the styryl protons, both pairs were confirmed to be *trans*-oriented, and two sets of doublet of doublet for the two pairs of proton on cyclobutane ring, HA, HA′ and HB, HB′ at δ 5.37 and 4.87 ($J_1 = 10.1$ Hz, $J_2 = 7.2$ Hz) was formed by a symmetrical *trans,trans*-AA′BB′ pattern. It indicates that **2a** was the *anti* head-to-tail form of photodimer.

In the mass spectrum of both **2b** and **3b**, the peak corresponding to asymmetrical cleavage of the cyclobutane ring is absent. Compounds **2b** and **3b** show same coupling pattern of protons on the cyclobutane ring with that of **2a** in ^{1}H NMR at δ 5.65 and 5.16 ($J_1 = 10.1$ Hz, $J_2 = 6.9$ Hz) for **2b**, and at 4.93 and 4.63 ($J_1 = 10.1$ Hz, $J_2 = 6.9$ Hz) for **3b**, respectively, which means that **2b** and **3b** have head-to-tail configuration of photodimer. From the differences of *J* value of two sets of styryl protons in ^{1}H NMR, **3b** (δ 6.97 and 6.54, d, d, 2H, 2H, $J = 12$ Hz) was *cis*-isomer of *trans*-**2b** (δ 7.86 and 7.72, d, d, 2H, 2H, $J = 15$ Hz). And the *cis–trans* isomerization from *trans*-**2b** to *cis*-**3b**, and from *cis*-**3b** to *trans*-**2b** is observed by irradiation of 365 nm and 290 nm UV light, respectively. Contrary to **2a**, **4b** shows asymmetrical cleavage of cyclobutane in mass spectra, *m/z* 490 and 182, which is indicative of 1,2-dipyridinyl-disubstituted cyclobutane. From the ^{1}H NMR, the ratio of 16H of aromatics to 8H of cyclobutanes and the pattern of proton on cyclobutane ring indicate that both sides of double bond of **1b** reacted in a head-to-head form. Characterization data for the photodimers are shown in below.

Compound **2a**: mass spectrum, *m/z* 668 (M^+), 424 ($-C_{15}H_8N_4$), 334 ($M^+/2$, symmetrical cleavage of cyclobutane), 257 ($M^+/2$ $-C_6H_5$); ^{1}H NMR ($CDCl_3$), δ 7.92 (d, 2H, $J = 15.4$ Hz), 7.69 (m, 4H), 7.54 (m, 6H), 7.18 (d, 2H, $J = 15.4$ Hz), 7.14 (s, 10H), 5.37 (dd, 2H, $J_1 = 10.1$ Hz, $J_2 = 7.2$ Hz), 4.87 (dd, 2H, $J_1 = 10.1$ Hz, $J_2 = 7.2$ Hz).

Compound **2b**: mass spectrum, *m/z* 672 (M^+), 427 ($-C_{15}H_8N_4$), 336 ($M^+/2$, symmetrical cleavage of cyclobutane), 258 ($M^+/2$ $-C_6H_5$); ^{1}H NMR ($CDCl_3$), δ 8.30, 8.28 (m, 2H), 8.25, 8.23 (m, 2H), 7.86 (d, 2H, $J = 15.0$ Hz), 7.76 (dt, 2H, $J_1 = 1.8$ Hz, $J_2 = 7.8$ Hz), 7.72 (d, 2H, $J = 15.0$ Hz), 7.40–7.28 (m, 8H), 6.99–6.94 (m, 2H), 5.65 (dd, 2H, $J_1 = 10.1$ Hz, $J_2 = 6.9$ Hz), 5.16 (dd, 2H, $J_1 = 10.1$ Hz, $J_2 = 6.9$ Hz).

Compound **3b**: mass spectrum, *m/z* 672 (M^+), 581 ($-C_6H_5N$), 427 ($-C_{14}H_7N_5$), 336 ($M^+/2$, symmetrical cleavage of cyclobutane), 258 ($M^+/2$ $-C_5H_4N$); ^{1}H NMR ($CDCl_3$), δ 8.07, 8.05 (m, 2H), 8.00, 7.98 (m, 2H), 7.58 (dt, 2H, $J_1 = 1.8$ Hz, $J_2 = 7.8$ Hz), 7.34 (dt, 2H, $J_1 = 1.8$ Hz, $J_2 = 7.8$ Hz), 7.23 (d, 2H, $J = 7.8$ Hz), 6.95–6.70 (m, 2H), 6.97 (d, 2H, $J = 12.0$ Hz), 6.94–6.89 (m, 2H), 6.73 (d, 2H, $J = 7.8$ Hz), 6.54 (d, 2H, $J = 12.0$ Hz), 4.93 (dd, 2H, $J_1 = 10.1$ Hz, $J_2 = 6.9$ Hz) 4.63 (dd, 2H, $J_1 = 10.1$ Hz, $J_2 = 6.9$ Hz).

Compound **4b**: mass spectrum, *m/z* 672 (M^+), 594 ($-C_5H_4N$), 490 (asymmetrical cleavage of cyclobutane), 427 ($-C_{14}H_7N_5$); ^{1}H NMR ($CDCl_3$), δ 8.56–8.55, 8.54–8.53 (m, 4H), 7.60 (dt, 4H, $J_1 = 1.8$ Hz, $J_2 = 7.5$ Hz), 7.27–7.26, 7.25–7.24 (m, 4H), 7.19–7.14 (m, 4H), 4.95–4.92 (m, 4H), 4.55–4.52 (m, 4H).

Acknowledgement

This research was supported by the Yeungnam University research grants in 2005.

References

[1] (a) Adams DM, Kerimo J, Olson EJC, Zaban A, Gregg BA, Barbara PF. J Am Chem Soc 1997;119:10608;
(b) Mizuguchi JJ. Appl Phys 1998;84:4479.
[2] (a) Higgins DA, Kerimo J, Bout DAV, Barbara PF. J Am Chem Soc 1996;118:4049;
(b) Yamamoto HM, Yamaura J-I, Kato R. J Am Chem Soc 1998;120:5905.
[3] (a) Wakelin LPG. Med Res Rev 1986;6:275;
(b) Shetty AS, Zhang J, Moore JS. J Am Chem Soc 1996;118:1019.
[4] Desiraju GR, Gavezzotti A. J Chem Soc Chem Commun 1989;621.
[5] (a) Hunter CA, Leighton P, Sanders JKM. J Chem Soc Perkin Trans 1 1989;547;
(b) Hamilton TD, Papaefstathiou GS, MacGillivray LR. J Solid State Chem 2005;178:2409.
[6] Zimmerman SC, Vanzyl CM, Hamilton GS. J Am Chem Soc 1989;111:1373.
[7] Hunter CA, Sanders JKM. J Am Chem Soc 1990;112:5525.
[8] Kazmaier PM, Hoffmann R. J Am Chem Soc 1994;116:9684.
[9] Inabe T, Mitsuhashi T, Maruyama Y. Bull Chem Soc Jpn 1998;61:4215.
[10] Lewis FD, Yang J-S, Stern CL. J Am Chem Soc 1996;118:2772.
[11] Dahne L. J Am Chem Soc 1995;117:12855.
[12] Kim JH, Matsuoka M, Fukunishi K. Dyes Pigments 1996;31:263.
[13] (a) Addadi L, Mil JV, Lahav M. J Am Chem Soc 1982;104:3422;
(b) Tanaka K, Toda F, Mochizuki E, Yasui N, Kai Y, Miyahara I, et al. Angew Chem Int Ed Engl 1999;38:3523;
(c) Toda F, Tanaka K, Tagi M. Tetrahedron 1987;43:1495.
[14] Tanaka K, Toda F. Chem Rev 2000;100:1025.
[15] (a) Enkelmann V. Adv Polym Sci 1984;63:91;
(b) Hasegawa M. Chem Rev 1983;83:507;
(c) Schwörer HEM, Huber R, Bloor D. Chem Phys Lett 1976;42:342;
(d) Xiao J, Yang M, Lauher JW, Fowler FW. Angew Chem Int Ed Engl 2000;39:2132;
(e) Foley JL, Li L, Sandman DJ, Vela MJ, Foxman BM, Albro R, et al. J Am Chem Soc 1999;121:7262.
[16] Kim JH, Hubig SM, Linderman SV, Kochi JK. J Am Chem Soc 2001;123:87.
[17] Novak K, Enkelmann V, Wegner G, Wagener KB. Angew Chem Int Ed Engl 1993;32:1614.
[18] (a) Cohen MD, Schmidt GMJ, Sonntag FI. J Chem Soc 1964, 1996, and 2000;
(b) Keating AE, Garcia-Garibay MA. In. Ramamurthy V, Schanze KS, editors. Organic and inorganic photochemistry. New York: Marcel Dekker; 1998. p. 195–248;
(c) Ramamurthy V, Venkatesan. Chem Rev 1987;87:433.
[19] (a) Desirraju GR, Sarma JARP. J Chem Soc Chem Commun 1983;45;
(b) Pokkuluri PR, Scheffer JR, Trotter J, Yap M. J Org Chem 1992;57:1486.
[20] Zimmerman H, Zuraw M. J Am Chem Soc 1989;111:7974.
[21] Leibovitch M, Olovsson G, Scheffer JR, Trotter J. J Am Chem Soc 1998;120:12755.
[22] (a) Appel WK, Jiang ZQ, Scheffer JR, Walsh L. J Am Chem Soc 1983;105:5354;
(b) Hosomi H, Ohba S, Tanaka K, Toda F. J Am Chem Soc 2000;122:1818.
[23] (a) Cohen MD. Angew Chem Int Ed Engl 1975;14:386;
(b) Gudmundsdottir AD, Lewis TJ, Randall LH, Scheffer JR, Rettig SJ, Trotter J, et al. J Am Chem Soc 1996;118:6167;
(c) Ariel S, Askari S, Evans SV, Hwang C, Jay J, Scheffer JR, et al. Tetrahedron 1987;43:1253.
[24] Ariel S, Askari S, Scheffer JR, Trotter J, Walsh L. J Am Chem Soc 1984;106:5726.
[25] (a) Stezowski JJ, Peachey NM, Goebel P, Eckhardt CJ. J Am Chem Soc 1993;115:6499;
(b) Peachey NM, Eckhardt CJ. J Am Chem Soc 1993;115:3519;
(c) Murthy GS, Arjunan A, Venkatesan K, Ramamurthy V. Tetrahedron 1987;43:1225.
[26] (a) Bosch E, Hubig SM, Lindeman SV, Kochi JK. J Org Chem 1998;63:592;
(b) Harris KDM, Thomas JM, Williams D. J Chem Soc Faraday Trans 1991;87(2):325;
(c) Wernick DL, Schochet S. J Phys Chem 1988;92:6773;
(d) Savion Z, Wernick DL. J Org Chem 1993;58:2424.
[27] (a) Kim JH, Matsuoka M, Fukunishi K. J Chem Res Synop 1999;132;
(b) Kim JH, Matsuoka M, Fukunishi K. Chem Lett 1999;143;
(c) Kim JH, Tani Y, Matsuoka M, Fukunishi K. Dyes Pigments 1999;43:7.
[28] Hasegawa M, Saigo K, Mori T, Uno H, Nohara M, Nakanishi H. J Am Chem Soc 1985;107:2788.
[29] Mizuguchi J, Rochat AC. J Imaging Sci 1988;32:135.
[30] (a) Ramasubbu N, Row TNG, Venkatesan K, Ramamurthy V, Rao CNR. J Chem Soc Chem Commun 1982;178;
(b) Gnanaguru K, Ramasubbu N, Venkatesan K, Ramamurthy V. J Org Chem 1985;50:2337.
[31] (a) Begley MJ, Crombie L, Knapp TFWB. J Chem Soc Perkin Trans 1 1979;976;
(b) Theocharis CR, Jones W, Thomas JM, Motevalli M, Hursthouse MB. J Chem Soc Perkin Trans 2 1984;71.
[32] Sarma JARP, Desiraju GR. J Chem Soc Perkin Trans 2 1985;1905.